Neutral and cationic paramagnetic amino-amidinate Iron(II) complexes

Sciarone, Timo J. J.; Nijhuis, Christian A.; Meetsma, Auke; Hessen, Bart

Published in:
Organometallics

DOI:
10.1021/om701155b

Publication date:
2008

Neutral and Cationic Paramagnetic Amino-amidinate Iron(II) Complexes: ^{19}F NMR Evidence for Interactions with Weakly Coordinating Anions

Timo J. J. Sciarone,[†,‡] Christian A. Nijhuis,[†] Auke Meetsma,[†] and Bart Hessen*[,†,‡]

Center for Catalytic Olefin Polymerization, Stratingh Institute for Chemistry and Chemical Engineering, University of Groningen, Nijenborgh 4, 9747 AG Groningen, The Netherlands, and Dutch Polymer Institute (DPI), P.O. Box 906, 5600 AX Eindhoven, The Netherlands

Received November 15, 2007

Two alkylamino-benzamidinates, $[RNC(Ph)NCH_2CH_2NMe_2]^-$ (^{Ar}L, R = 2,6-*i*Pr$_2$C$_6$H$_3$; ^{Si}L, R = SiMe$_3$), have been employed as ligands for Fe(II). The ligands adopt bridging coordination modes in their diiron(II) dichloro complexes $[(\mu\text{-}^{R}L)FeCl]_2$ (**1**). Their structure and reactivity are strongly dependent on the nature of R. With CO, $[(\mu\text{-}^{Ar}L)FeCl]_2$ (**1a**) forms the monomeric, 18-electron dicarbonyl compound $[\kappa^3\text{-}C(O)(2,6\text{-}iPr_2C_6H_3)NC(Ph)NCH_2CH_2NMe_2]FeCl(CO)_2$ (**3**), in which CO has inserted into the Fe−N(amidinate) bond, whereas $[(\mu\text{-}^{Si}L)FeCl]_2$ (**1b**) is unreactive under similar conditions. Alkylation of **1a** was unsuccessful, leading to ligand redistribution and isolation of $(\kappa^2\text{-}^{Ar}L)_2Fe$ (**2**), in which the ligands adopt a κ^2-amido-amino coordination mode, but **1b** reacts with KCH_2Ph to give the 14-electron diiron dibenzyl derivative $[(\mu\text{-}^{Si}L)FeCH_2Ph]_2$ (**4**). Benzyl abstraction by $B(C_6F_5)_3$, $[Ph_3C][B(C_6F_5)_4]$, or $[PhNHMe_2][B(C_6F_5)_4]$ affords the paramagnetic monocation $[(\mu\text{-}^{Si}L)_2Fe_2CH_2Ph]^+$ (**5**$^+$) partnered with $[PhCH_2B(C_6F_5)_3]^-$ or $[B(C_6F_5)_4]^-$, respectively. Interactions of these weakly coordinating anions with the paramagnetic Fe(II) centers in solution are apparent from significantly shifted and broadened resonances in the ^{19}F NMR spectra.

Introduction

Iron(II) complexes supported by neutral pyridine-2,6-diimine ligands have emerged as highly active precatalysts for olefin polymerization when activated with methylaluminoxane (MAO) cocatalyst.[1] Electronically unsaturated, 14 valence electron (14 VE), cationic iron alkyls have been identified as competent catalytically active species in this transformation.[2] In cationic transition metal alkyl catalysts, the metal center is influenced by the coordinative properties of the counterion. This can influence, to a significant extent, activity, stability, chain transfer characteristics, and stereoselectivity of the catalytic system.[3] In non-MAO-activated catalysts, perfluorinated arylborates, such as $[B(C_6F_5)_4]^-$, are often employed as counterions, since they are among the most weakly coordinating anions available.

Chart 1

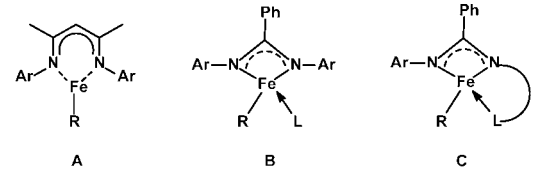

Monoanionic, sterically hindered β-diketiminate ligands have been utilized to stabilize electron-deficient (12 VE), neutral Fe(II) monoalkyls.[4,5] Although these neutral, paramagnetic systems are inactive for olefin polymerization, we observed that the derived cations allowed spectroscopic observations of cation−anion interactions in solution involving weakly coordinating fluorinated arylborate anions.[5] The paramagnetic cation acts as a chemical shift reagent, causing significant effects on the ^{19}F NMR spectra of the associated anions.

A more open coordination space around the metal center is expected to enhance the extent of cation−anion interactions. Since amidinates, $[R'C(NR)_2]^-$, are isoelectronic with β-diketiminates, but have considerably smaller N−M−N bite angles in their transition metal complexes, these compounds ususally feature a more accessible metal center. Whereas 12 VE Fe(II) monoalkyls [(N^N)FeR] (N^N = monoanionic κ^2 ligand) are readily isolated for the β-diketiminate ligand (**A**, Chart 1), those supported by the smaller amidinate ligand were found to be unstable with respect to ligand redistributions forming the bis(amidinate) complex $[(N^N)_2Fe]$. The mono(amidinate) complexes could be stabilized, however, through coordination of an additional Lewis base L, thus allowing for isolation of an

* Corresponding author. E-mail: B.Hessen@rug.nl.
† University of Groningen.
‡ DPI.

(1) (a) Britovsek, G. J. P.; Gibson, V. C.; Kimberley, B. S.; Maddox, P. J.; McTavish, S. J.; Solan, G. A.; White, A. J. P.; Williams, D. J. *Chem. Commun.* **1998**, 849. (b) Small, B. L.; Brookhart, M.; Bennett, A. M. A. *J. Am. Chem. Soc.* **1998**, *120*, 4049. (c) Britovsek, G. J. P.; Bruce, M.; Gibson, V.; Kimerley, B. S.; Maddox, P. J.; Mastroianni, S.; McTavish, S. J.; Redshaw, C.; Solan, G. A.; Strömberg, S.; White, A. J. P.; Williams, D. J. *J. Am. Chem. Soc.* **1999**, *121*, 8728. (d) Ittel, S. D.; Johnson, L. K.; Brookhart, M. *Chem. Rev.* **2000**, *100*, 1169. (e) Mecking, S. *Angew. Chem., Int. Ed.* **2001**, *40*, 534. (f) Gibson, V. C.; Spitzmesser, S. K. *Chem. Rev.* **2003**, *103*, 283.

(2) Bouwkamp, M. W.; Lobkovsky, E.; Chirik, P. J. *J. Am. Chem. Soc.* **2005**, *127*, 9660.

(3) Chen, E.Y.-X.; Marks, T. J. *Chem. Rev.* **2000**, *100*, 1391.

(4) (a) Andres, H.; Bominaar, E. L.; Smith, J. M.; Eckert, N. A.; Holland, P. A.; Münck, E. *J. Am. Chem. Soc.* **2002**, *124*, 3012. (b) Smith, J. M.; Lachicotte, R. J.; Holland, P. L. *Organometallics* **2002**, *21*, 4808. (c) Vela, J.; Smith, J. M.; Lachicotte, R. J.; Holland, P. L. *Chem. Commun.* **2002**, 2886. (d) Vela, J.; Vaddadi, S.; Cundari, T. R.; Smith, J. M.; Gregory, E. A.; Lachicotte, R. J.; Flaschenriem, C. J.; Holland, P. L. *Organometallics* **2004**, *23*, 5226.

(5) (a) Sciarone, T. J. J.; Meetsma, A.; Hessen, B.; Teuben, J. H. *Chem. Commun.* **2002**, 1580. (b) Sciarone, T. J. J.; Meetsma, A.; Hessen, B. H. *Inorg. Chim. Acta* **2006**, *359*, 1815.

10.1021/om701155b CCC: $40.75
Publication on Web 04/11/2008

Scheme 1

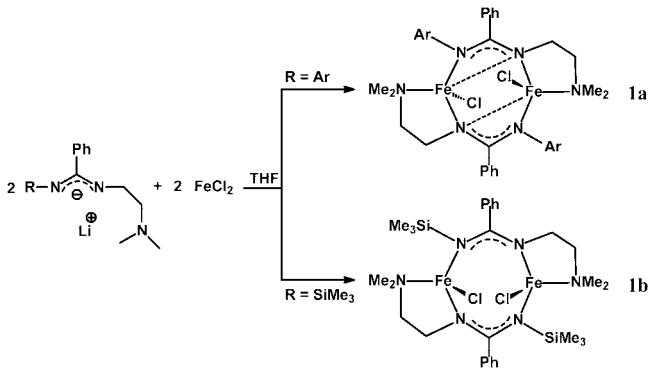

Fe(II) alkyl of the type [(N^N)FeR(L)] (**B**, Chart 1).[6] Enhanced stability is therefore expected for Fe(II) monoalkyls chelated by amidinate ligands functionalized with a pendant Lewis base (**C**, Chart 1). Amidinates functionalized with amine or pyridine functionalities on one of the nitrogen atoms have been reported as ancillary ligands for various transition metals, lanthanides, and main group elements.[7–11]

Here we describe the chemistry of two dimethylaminoethyl-substituted benzamidinates, $[RNC(Ph)NCH_2CH_2NMe_2]^-$ (^{Ar}L, R = Ar, and ^{Si}L, R = $SiMe_3$) with Fe(II), including the isolation of a 14 VE diiron dibenzyl complex. Subsequent benzyl abstraction affords ion pairs, which provide an opportunity to observe very weak cation−anion interactions between a paramagnetic diiron cation and (perfluoroaryl)borate anions by means of ^{19}F NMR spectroscopy.

Results and Discussion

Synthesis and Characterization of Amidinate-amine Iron(II) Chlorides. The lithium amidinates Li[^{R}L] react with 1 equiv of $FeCl_2$ in THF solvent to afford the paramagnetic diiron complexes [(μ-^{Ar}L)FeCl]$_2$ (**1a**) and [(μ-^{Si}L)FeCl]$_2$ (**1b**) in 40% and 64% isolated yields, respectively (Scheme 1). Complex **1a** is soluble in THF and toluene, while **1b** is sparingly soluble in THF or dichloromethane.

The molecular structures of both diiron complexes were determined by X-ray diffraction (Figures 1 and 2). Dimer **1a** is lying on a crystallographic inversion center, whereas **1b** has crystallographic C_2-symmetry.

In both complexes, the iron centers are bridged by the amidinate part of the ligand, and the dimethylamino donor forms a five-membered chelate ring including the amidinate nitrogen atom carrying this functionality. The amidinate nitrogen atoms carrying the R-subsituents are essentially planar (**1a**: $\sum_{N1}$ = 358.58°, **1b**: $\sum_{N3}$ = 359.95°). Whereas bridging amidinates often form so-called lantern complexes (e.g., [μ-$HC(NPh)_2]_nFe_2$, n = 3 or 4), showing Fe−Fe bonds in the range 2.23−2.46 Å,[12,13] the Fe−Fe separations in dimers **1** (**1a**: 2.9242(6) Å, **1b**: 3.0792(10) Å) do not indicate the presence of a direct Fe−Fe interaction. Despite the overall similarities, the different R

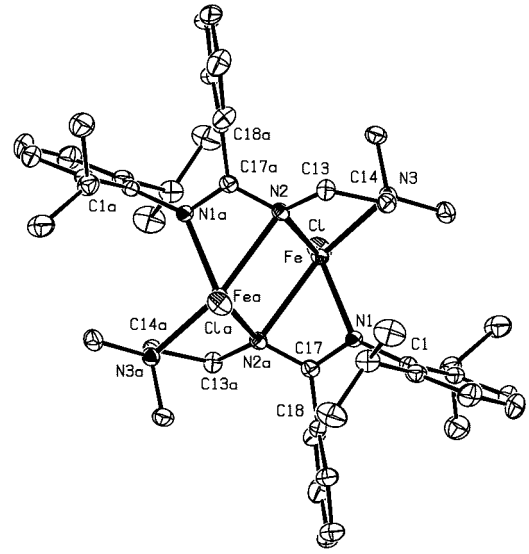

Figure 1. Crystal structure of **1a**. Thermal ellipsoids are drawn at 50% probability. Hydrogen atoms have been omitted for clarity. Selected interatomic bond distances (Å) and angles (deg): Fe−Fe_a 2.9242(6), Fe−N1 2.090(2), Fe−N2 2.136(2), Fe−N3 2.160(2), Fe−N2_a 2.390(2), Cl−Fe−N1 106.84, Cl−Fe−N2 136.40(7), Cl−Fe−N3 101.92(6), Cl−Fe−N2_a 91.12(5), N1−Fe−N2 115.19(9), N1−Fe−N2_a 60.02(8), N1−Fe−N3 105.10(9), N2−Fe−N3 (78.46(8), N2_a−Fe-N2 99.71(8), N2_a−Fe-N3 162.94(8).

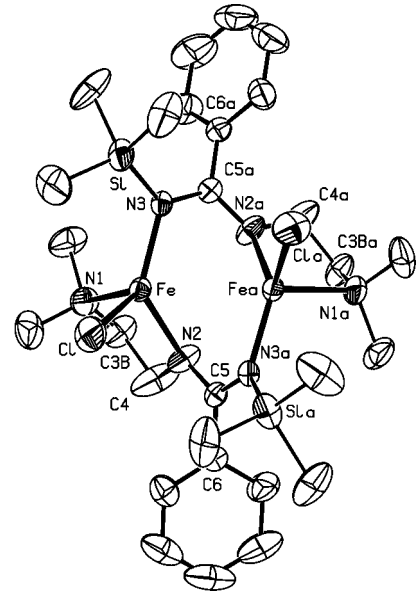

Figure 2. Crystal structure of **1b**. Thermal ellipsoids are drawn at 50% probability. Hydrogen atoms have been omitted for clarity. Selected interatomic bond distances (Å) and angles (deg): Fe−Fe_a 3.0792(10), Fe−N1 2.193(4), Fe−N2 2.061(3), Fe−N3 2.024(3), Cl−Fe−N1 105.18(10), Cl−Fe−N2 101.84(10), Cl−Fe−N3 122.32(8), N1−Fe−N2 80.94(12), N1−Fe−N3 106.38(11), N2−Fe−N3 129.85(12).

(6) Sciarone, T. J. J.; Nijhuis, C. A.; Meetsma, A.; Hessen, B. *Dalton Trans.* **2006**, 4896.
(7) Brandsma, M. J. R.; Brussee, E. A. C.; Meetsma, A.; Hessen, B.; Teuben, J. H. *Eur. J. Inorg. Chem.* **1998**, 1867.
(8) Doyle, D.; Gun'ko, Y. K.; Hitchcock, P. B.; Lappert, M. F. *J. Chem. Soc., Dalton Trans.* **2000**, 4093.
(9) (a) Bambirra, S.; Brandsma, M. J. R.; Brussee, E. A. C.; Meetsma, A.; Hessen, B.; Teuben, J. H. *Organometallics* **2000**, *19*, 3197. (b) Bambirra, S.; Otten, E.; van Leusen, D.; Meetsma, A.; Hessen, B. *Z. Anorg. Allg. Chem.* **2006**, *632*, 1950.
(10) Kincaid, K.; Gerlach, C. P.; Giesbrecht, G. R.; Hagadorn, J. R.; Whitener, G. D.; Shafir, A.; Arnold, J. *Organometallics* **1999**, *18*, 5360.
(11) Boyd, C. L.; Guiducci, A. E.; Dubberley, S. R.; Tyrrell, B. R.; Mountford, P. *J. Chem. Soc., Dalton Trans.* **2002**, 4175.
(12) (a) Cotton, F. A.; Daniels, L. M.; Falvello, L. R.; Matonic, J. H.; Murillo, C. A. *Inorg. Chim. Acta* **1997**, *256*, 269. (b) Cotton, F. A.; Daniels, L. M.; Falvello, L. R.; Murillo, C. A. *Inorg. Chim. Acta* **1994**, *219*, 7.
(13) Cotton, F. A.; Daniels, L. M.; Matonic, J. H.; Murillo, C. A. *Inorg. Chim. Acta* **1997**, *256*, 277.

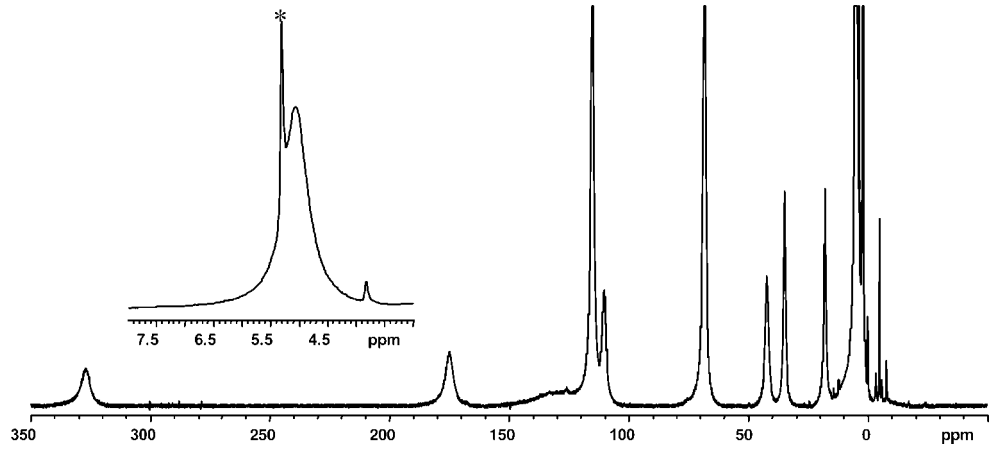

Figure 3. ^{1}H NMR spectrum of **1b** (500 MHz, CD_2Cl_2, RT). Asterisk (inset) indicates $CDHCl_2$.

substituents in the ligands result in some significant differences in molecular geometry for the dinuclear complexes. In **1b** each amidinate nitrogen is bound to only one iron atom, whereas in **1a** the amidinate nitrogen atom bearing the dimethylaminoethyl substituent (N2) is bridging the iron centers, with one shorter (2.136(2) Å) and one longer (2.390(2) Å) Fe−N bond. In **1a** the two bridging nitrogen atoms and the iron atoms thus form a planar Fe_2N_2 diamond motif. A bonding situation similar to that in **1a** was found in the dinuclear aminoamidinate lithium complex $\{[\mu\text{-}Me_3SiNC(Ph)N(CH_2)_3NMe_2]Li\}_2$.[8] For Fe(II), a related structure is present in the dimeric bis(amidinate) complex $\{[\kappa^2\text{-}PhC(NPh)_2][\mu\text{-}PhC(NPh)_2]Fe\}_2$.[13] While the amidinate NCN planes of the two ligands in **1a** have parallel orientations, those in **1b** are inclined at 82.3(5)°. A final significant structural difference between the dimers **1a** and **1b** is that in **1a** the chlorides display a *trans*-arrangement relative to the $Fe_2(\mu$-amidinate$)_2$ unit, whereas in **1b** they display a *cis*-arrangement. The *cis*-orientation found in **1b** is likely to result in a higher dipole moment, which is reflected in the low solubility of this compound in apolar solvents.

Dimers **1** are paramagnetic with room-temperature magnetic moments of 5.3 μ_B (**1a**) and 5.0 μ_B (**1b**) per iron ion, indicating a high-spin ($S = 2$) configuration for Fe(II). The high-spin nature of the chloro complexes is also evident from their ^{1}H NMR spectra. The spectrum of **1a** in C_6D_6 displays nine resonances in a window from δ 110 to −40 ppm with linewidths ranging from 30 to 4500 Hz. Complex **1b** shows 10 signals from 350 to 0 ppm with linewidths ($\Delta\nu_{1/2}$) ranging from 47 to 9600 Hz in CD_2Cl_2. For both complexes, some resonances are too broad to be observed, and extreme broadness of some of the observable peaks makes their integration unreliable. This precludes unambiguous assignment of the resonances for **1a**, but the spectrum is nevertheless useful as a fingerprint. For the spectrum of **1b** (Figure 3) however, some tentative assignments could be made.

The resonance at 5.1 ppm is assigned to the protons of the silyl groups (18H). The appearance of two 6H resonances at 115.3 and 68.5 ppm for the NCH_3 protons suggests coordination of the amino groups. Amino coordination also makes the four methylene protons of the ligand diastereotopic. Two pairs of resonances (2H each) from these protons are found at δ 327.0 ($\Delta\nu_{1/2} = 2130$ Hz), 175.1 (1820 Hz), 110.5 (990 Hz), and 42.4 (790 Hz) ppm. The *meta* protons of the phenyl group are observed as two signals at 35.1 and 18.1 ppm (both 490 Hz), each integrating for 2H, suggesting that rotation of this group is slow on the NMR time scale. Finally, the *para* protons resonate at 2.2 ppm (47 Hz). A resonance for the phenyl *ortho* protons is not observed, presumably due to their proximity to the paramagnetic Fe(II) centers.

Scheme 2

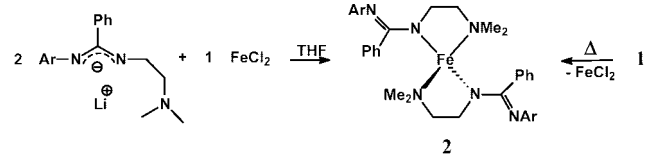

Thermal Stability. The two dinuclear amidinate-amine iron complexes **1a** and **1b** show a significant difference in thermal stability. Whereas the Me_3Si-substituted **1b** is stable in solution at ambient temperature for days, monitoring solutions of **1a** in C_6D_6 or PhMe-d_8 by ^{1}H NMR spectroscopy shows that the complex is fully converted into a new paramagnetic species within one day at room temperature.

It turned out that this thermolysis product is the mononuclear 2:1 complex $(^{Ar}L)_2Fe$ (**2**), which was also prepared directly by the reaction of $FeCl_2$ with 2 equiv of Li[^{Ar}L] in THF (Scheme 2). Complex **2** was characterized by microanalysis, ^{1}H NMR and IR spectroscopy, and single-crystal X-ray diffraction.

The molecular structure of **2** (Figure 4) shows that the amino-amidinate ligands are bound in a κ^2-amino-amido fashion, leaving the arylimine moiety uncoordinated. Consistently, the IR spectrum shows a strong C=N absorption at 1578 cm^{-1}. Apparently, decoordination of the imine is more favorable than that of the pendant amine, possibly due to reduction of steric hindrance around the metal center. The iron center is coordinated in a distorted tetrahedral fashion, with the N−Fe−N coordination planes inclined at 85.42(8)°. The average N−Fe−N bite angle of the amino-amido ligands is 82°.

Complex **1b** decomposes upon heating at 50 °C for several days (or 24 h at 80 °C), but the identity of the decomposition product(s) could not be established. The ^{1}H NMR spectrum of the mixture shows an intense signal at δ 0.00 ppm, suggesting loss of the $SiMe_3$ group.

Reaction with CO. In spite of the formal electron deficiency of complexes **1** (14 VE per Fe), their high-spin nature leaves no empty valence orbitals available. Thus, complexes **1** are unreactive toward simple Lewis bases such as THF or PMe_3. Nevertheless, complex **1a** does react with the typical π-acceptor ligand CO. Exposure of **1a** to excess CO (1 atm) in toluene solution cleanly affords the 18 VE carbonyl derivative [κ^3-C(O)(2,6-*i*$Pr_2C_6H_3$)NC(Ph)$NCH_2CH_2NMe_2$]FeCl$(CO)_2$ (**3**), which was isolated in 81% yield (Scheme 3). The identity of **3** was established by X-ray diffraction.

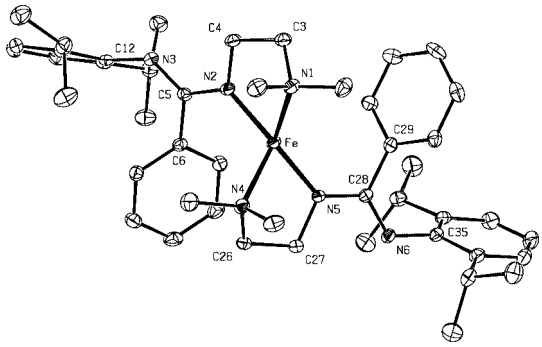

Figure 4. Xray structure of **2**. Thermal ellipsoids are drawn at 50% probability. Selected interatomic bond distances (Å) and angles (deg): Fe−N1 2.1861(14), Fe−N2 2.0018(13), Fe−N4 2.1905(15), Fe−N5 1.9924(13), N2−C5 1.357(2), N3−C5 1.300(2), N5−C28 1.348(2), N6−C28 1.303(2), N1−Fe−N2 82.75(5), N1−Fe−N4 105.96(5), N1−Fe−N5 127.31(6), N2−Fe−N4 118.55(6), N2−Fe−N5 140.22(6), N4−Fe−N5 81.18(5).

Scheme 3

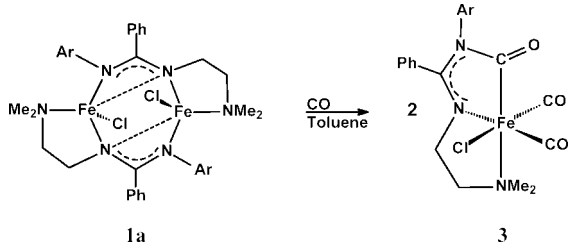

1a **3**

Complex **3** results from the insertion of a CO molecule into one of the amidinate-N−Fe bonds, which converts the amidinate into a carbamoyl functionality, and saturation of the Fe(II) center with two CO ligands. Related CO insertions have been reported for $[PhC(NAr)_2]FeCl(\mu\text{-}Cl)Li(THF)_3$[6] and $[FcC(NCy)_2]CpFe(CO)$ (Fc = ferrocenyl).[14] In contrast to **1a**, complex **1b** does not react with CO under identical conditions. Bis(aminoamidinate) complex **2** also does not react with CO under the applied conditions, whereas the homoleptic amidinate complexes $[t\text{BuC}(NR)_2]_2Fe$ (R = Cy, *i*Pr) react with CO only to give the bis(carbonyl) adducts $[t\text{BuC}(NR)_2]_2Fe(CO)_2$ without subsequent CO insertion.[15] This is also the case for the dinuclear amidinate complex $\{[\mu\text{-}1,2\text{-}[NC(Ph)NSiMe_3]_2\text{-}c\text{-}C_6H_{10}]Fe\}_2$.[16]

The X-ray structure of **3** (Figure 5) shows a pseudo-octahedrally coordinated iron center, with the amino-carbamoyl ligand occupying a meridional coordination mode.

The difference in Fe−C bond length (0.05 Å) for the terminal carbonyls reflects the stronger *trans* influence of the amide versus the chloride ligand. The carbamoyl chelate ring is almost planar, as indicated by the sums of the angles around the nonmetal atoms, which all approach 360° (highest deviation = 0.5° for N3), suggesting significant conjugation within the chelate. Nevertheless, the C5−N distances differ by about 0.11 Å, indicating some extent of localization.

The IR spectrum of **3** is consistent with the solid state structure, showing absorptions at 2037 and 1949 cm^{-1} for the terminal carbonyls, while the carbamoyl carbonyl absorbs at 1669 cm^{-1}. Complex **3** is diamagnetic, and shows ^1H and $^{13}C\{H\}$ NMR spectra consistent with the C_1-symmetry observed in the solid state. The spectra give evidence of hindered rotation of the 2,6-*i*$Pr_2C_6H_3$ ring about the C_{ipso}−N bond. Coordination of the amino arm in solution is indicated by the presence of two resonances for the NMe groups. The three carbonyl functions show resonances at δ 208.1, 207.9, and 207.5 ppm (absolute assignments were not made).

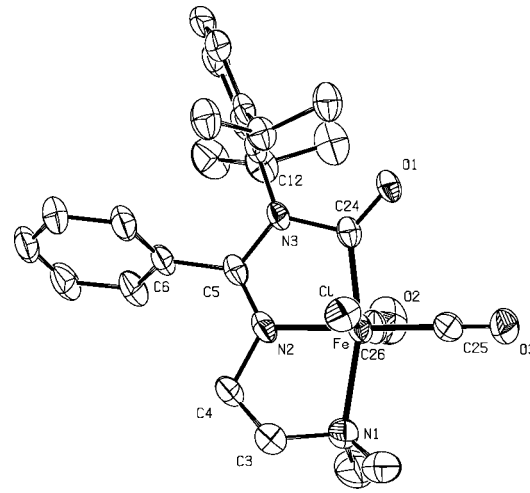

Figure 5. X-ray structure of **3**. Thermal ellipsoids are drawn at 50% probability. Hydrogens and cocrystallized THF molecules have been omitted for clarity. Selected interatomic distances (Å) and angles (deg): Fe−C24 1.942(3), Fe−C25 1.790(3), Fe−C26 1.845(3), Fe−N1 2.146(3), Fe−N2 1.935(2), C24−N3 1.453(3), N3−C5 1.393(3), N2−C5 1.283(3).

Scheme 4

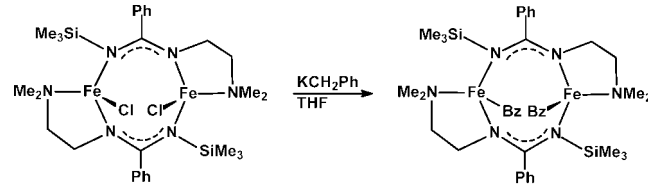

1b **4**

Alkylation. Alkylation of chloro complex **1a** was investigated using LiMe, $LiCH_2SiMe_3$, $LiCH(SiMe_3)_2$, KCH_2Ph, and $PhCH_2MgBr$ in THF at −80 °C. Nevertheless, in all cases, dark brown to black reaction mixtures were formed, and pentane extraction resulted only in the isolation (in 20−50% yield based on Fe) of $(^{Ar}L)_2Fe$ (**2**), as identified by ^1H NMR. GC-MS analysis of the reaction mixture indicated the formation of 1,2-diphenylethane when KCH_2Ph was employed as the alkylating agent. These observations suggest that an initially formed benzyl complex decomposes via ligand redistribution to form **2** and "$Fe(CH_2Ph)_2$". In the absence of strong monodentate[17] or chelating bidentate[18] donor ligands, the latter is unstable with respect to Fe(0) and $PhCH_2CH_2Ph$. Similar decomposition products were found previously upon attempted synthesis of Fe(II) monoalkyls supported by the nonfunctionalized amidinate ligand $[PhC(NAr)_2]^-$.[6]

Alkylation of **1b** using LiMe or $LiCH_2SiMe_3$ in THF at −40 °C also led to decomposition to give black reaction mixtures. With $PhCH_2MgBr$, a red solution was obtained initially, but subsequent workup still resulted in decomposition with formation of $PhCH_2CH_2Ph$. Nevertheless, the reaction of **1b** with

(14) Hagadorn, J. R.; Arnold, J. *J. Organomet. Chem.* **2001**, *637−639*, 521.

(15) Vendemiati, B.; Prini, G.; Meetsma, A.; Hessen, B.; Teuben, J. H.; Traverso, O. *Eur. J. Inorg. Chem.* **2001**, 707.

(16) Kawaguchi, H.; Matsuo, T. *Chem. Commun.* **2002**, 958.

(17) Cámpora, J.; Naz, A. M.; Palma, P.; Álvarez, E.; Reyes, M. L. *Organometallics* **2005**, *24*, 4878.

(18) Hermes, A. R.; Girolami, G. S. *Organometallics* **1987**, *6*, 763.

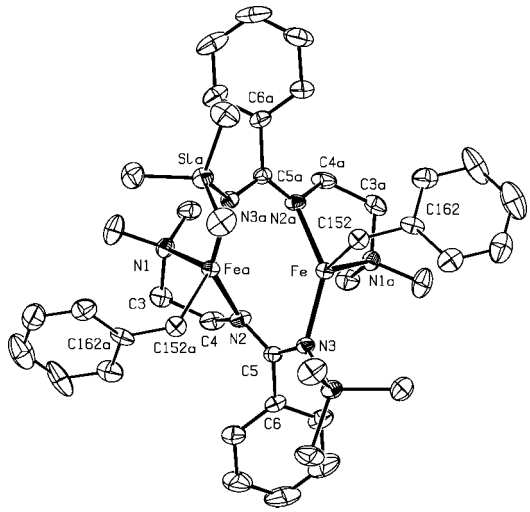

Figure 6. X-ray structure of **4** (dominant conformer shown). Thermal ellipsoids are drawn at 50% probability. Selected interatomic distances (Å) and angles (deg): Fe−Fe_a 3.0189(6), Fe−C152 2.087(6), Fe−N1 2.235(2), Fe−N2 2.099(2), Fe−N3 2.055(2), C152−Fe−N1 114.88(14), C152−Fe−N2 96.14(13), C152−Fe−N3 120.50(14), N1−Fe−N2 79.23(8), N1−Fe−N3 102.35(8), N2−Fe−N3 136.71(9).

KCH_2Ph in THF at −40 °C afforded the diiron dibenzyl complex $[(\mu\text{-}^{Si}L)FeCH_2Ph]_2$ (**4**), which was isolated in 43% yield as red crystals after recrystallization from toluene (Scheme 4).

The successful isolation of **4** from the reaction of **1b** with KCH_2Ph shows that problems in alkylation of **1b** with organolithium and Grignard reagents are not due to intrinsic instability of **4**. Possibly, the Li^+ and Mg^{2+} cations introduced by these reagents compete with Fe(II) for the aminoamidinate ligands, leading to ligand redistribution. Although direct evidence for the formation of Li or Mg aminoamidinate complexes not was obtained in this case, encapsulation of Li by the amino functions of two ^{Si}L ligands has been observed in the yttriates $Li[(\mu\text{-}^{Si}L)_2Y(CH_2R)_2]$ ($R = SiMe_3$, Ph).[9a]

The crystal structure of **4** (Figure 6) resembles that of the parent chloride **1b**. The *cis*-orientation of the chlorides in the starting material is translated into a *cis*-orientation of the benzyl groups in **4**. The iron carbon bond length (2.087(6) Å) in **4** is only slightly shorter than that in the bis(*p*-tolyl) complex (dippe)$Fe(CH_2C_6H_4Me)_2$ (dippe = 1,2-(diisopropylphosphino)-ethane) (Fe−C = 2.120(6) Å).[18]

The benzyl methylene hydrogens could not be located in X-ray structure due to disorder of the benzyl fragments, which were refined in two orientations (see Experimental Section). Nevertheless, the $Fe-CH_2-C_{ipso}$ angles (114.4(3)° and 112.4(3)°) in these conformations rule out secondary interactions between the benzyl groups and the iron centers. This is consistent with the absence of empty valence orbitals on the four-coordinate, 14 VE electron iron centers, given the high-spin ($S = 2$) spin state (*vide infra*).

Like its chloro precursor, benzyl derivative **4** is paramagnetic, possessing a room-temperature magnetic moment of 5.8 μB per iron ion, consistent with high-spin ($S = 2$) iron centers. The paramagnetic ^1H NMR spectrum of **4** in C_6D_6 contains 11 broad resonances in the δ +200 to −75 ppm window at positions very different from those of **1b**. Despite the structural similarity to its chloride precursor, the ligand resonances of **4** could not be assigned unambiguously. However, characteristic resonances at δ 30.4, −41.2, and −60.0 ppm could be assigned to the *meta*, *ortho*, and *para* protons, respectively, of the benzyl group. The benzyl groups in tetrahedral, high-spin Fe(II) dibenzyl compounds $(L_2)Fe(CH_2Ph)_2$ (L = Lewis base) exhibit comparable chemical shifts.[19] The benzyl α-protons of **4** are not observed in the spectrum, presumably due to extreme line broadening resulting from their proximity to the paramagnetic iron centers.

Cation−Anion Interactions. Abstraction of one of the benzyl ligands of **4** by Lewis or Brønsted acids in C_6D_5Br solution generates the monocation $[(\mu\text{-}^{Si}L)_2Fe_2CH_2Ph]^+$ (**5**$^+$) (Scheme 5). These reactions are accompanied by a color change from yellow to dark red. The paramagnetism of **5**$^+$ in combination with its low symmetry results in rather uninformative ^1H NMR spectra consisting of many broad and in part overlapping resonances. ^{19}F NMR spectroscopy proved to be more useful for study of the ion pairs.

Abstraction of the benzyl ligand by $B(C_6F_5)_3$ was confirmed by the presence of the $[PhCH_2B(C_6F_5)_3]^-$ ion ($m/z = -603$) as the parent ion in the negative-ion ES mass spectrum. The ^{19}F NMR spectum of ion pair [**5**][$PhCH_2B(C_6F_5)_3$] (Figure 7a) shows three broad lines with 2:2:1 integral ratios. Remarkably, the *p*-F resonance is found *upfield* from the *m*-F resonance, an observation made previously with paramagnetic β-diketiminate Fe(II) cations.[4b] The spectral data suggest that [**5**][$PhCH_2B(C_6F_5)_3$] in bromobenzene solution is at least partly present as a contact ion pair in which **5**$^+$ acts as a paramagnetic shift reagent for the anion. In the absence of an X-ray structure for the ion pair, the bonding mode for the [$PhCH_2B(C_6F_5)_3$] anion cannot be established, but π-coordination of the phenyl moiety is well-precedented.[3,20]

Addition of excess Lewis base (THF, pyridine) induces a color change from dark red to yellow and converts the ^{19}F NMR spectrum into three sharp resonances (Figure 7b), with shifts characteristic for the free $[PhCH_2B(C_6F_5)_3]^-$ ion.[21] Evidently, the Lewis base displaces the borate anion from the Fe(II) center, disrupting the interaction between the paramagnetic cation and the anion.

It is not clear whether contact ion pair [**5**][$PhCH_2B(C_6F_5)_3$] in C_6D_5Br is in equilibrium with a solvent-separated ion pair. The ^{19}F NMR spectrum −35 °C still features only three signals, indicating that, if there is reversible association/dissociation of the anion with the metal center, the process is still fast on the NMR time scale.

Generation of cation **5**$^+$ partnered with the less nucleophilic $[B(C_6F_5)_4]^-$ ion was effected by reaction of **4** with the corresponding triphenylcarbenium or *N*,*N*-dimethylanilinium salts. The expected coproducts, 1,1,1,2-tetraphenylethane and *N*,*N*-dimethylanilline/toluene, respectively, were detected by ^1H NMR and GC-MS. The ^{19}F NMR spectrum of [**5**][$B(C_6F_5)_4$] generated from **4** and [Ph_3C][$B(C_6F_5)_4$] (Figure 8a) shows three broad resonances. They are somewhat less broadened than for [**5**][$PhCH_2B(C_6F_5)_3$], and the *p*-F resonance is now found slightly downfield from the *m*-F resonance. A very similar spectrum is obtained by the protonolytic route using [$PhNHMe_2$][$B(C_6F_5)_4$], suggesting that the $PhNMe_2$ coproduct does not significantly coordinate to the cation.[22] Although the ^{19}F

(19) (a) Hermes, A. R.; Girolami, G. S. *Organometallics* **1987**, *6*, 763. (b) Hill, D. H.; Sen, A. *J. Am. Chem. Soc.* **1988**, *110*, 1650. (c) Hill, D. H.; Parvez, M. A.; Sen, A. *J. Am. Chem. Soc.* **1994**, *116*, 2889. (d) Bart, S.; Hawrelak, E. J.; Schmisseur, A. K.; Lobkovsky, E.; Chirik, P. J. *Organometallics* **2004**, *23*, 237.

(20) (a) Pellecchia, C.; Grassi, A.; Immirzi, A. *J. Am. Chem. Soc.* **1993**, *115*, 1160. (b) Pellecchia, C.; Immirzi, A.; Grassi, A.; Zambelli, A. *Organometallics* **1993**, *12*, 4473. (c) Lee, L. W. M.; Piers, W. E.; Elsegood, M. R. J.; Clegg, W.; Parvez, M. *Organometallics* **1999**, *18*, 2947.

(21) (a) Horton, A. D.; de With, J.; van der Linden, A.; van de Weg, H. *Organometallics* **1996**, *15*, 2672. (b) Horton, A. D.; de With, J. *Organometallics* **1997**, *16*, 5424.

Scheme 5

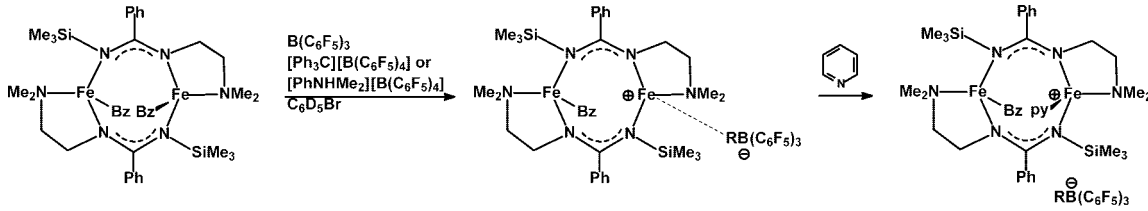

4 [5][RB(C6F5)3] [5(py)][R(B(C6F5)3]

NMR spectra suggest looser ion pairing for [**5**][$B(C_6F_5)_4$] than for [**5**][$PhCH_2B(C_6F_5)_3$], interaction of $[B(C_6F_5)_4]^-$ with the paramagnetic cation $\mathbf{5}^+$ is clearly demonstrated by the addition of pyridine. Reaction with the Lewis base results in a color change from dark red to bright yellow and a ^{19}F NMR spectrum characteristic of the free $[B(C_6F_5)_4]^-$ ion (Figure 8b).

Upon cooling a solution of [**5**][$B(C_6F_5)_4$] in C_6D_5Br to −30 °C, the *p*-F resonance shifts upfield from the *m*-F resonance, consistent with stronger ion pairing at low temperature. Nevertheless, the four C_6F_5 rings remain magnetically equivalent at this temperature, indicating rapid interconversion. Therefore, the mode of the interaction between $\mathbf{5}^+$ and $[B(C_6F_5)_4]^-$ in solution cannot be inferred with certainty from the spectra. Whereas for [**5**][$B(C_6F_5)_4$], the largest effect is seen on the chemical shifts of the *m*-F and *p*-F atoms, there is also precedent for interaction of this anion through the *o*-F and *m*-F atoms

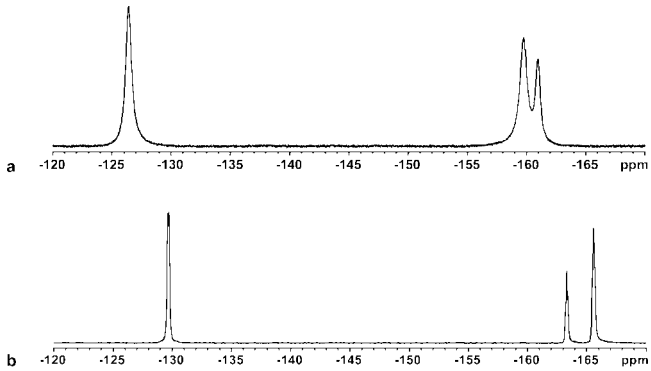

Figure 7. ^{19}F NMR spectra (188 MHz, C_6D_5Br, RT) of **4** + $B(C_6F_5)_3$ (a) and **4** + $B(C_6F_5)_3$ + pyridine-d_5 (b).

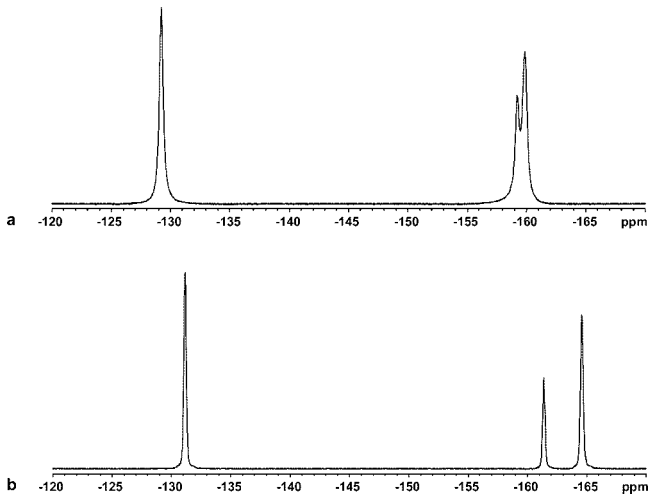

Figure 8. ^{19}F NMR spectra (188 MHz, C_6D_5Br, RT) of **4** + $[Ph_3C][B(C_6F_5)_4]$ (a) and **4** + $[Ph_3C][B(C_6F_5)_4]$ + pyridine-d_5 (b).

(e.g., in $[Cp^*_2ThMe][B(C_6F_5)_4]$ inferred from ^{19}F,^1H HOESY NMR experiments in C_6D_6[23]).

The role of the solvent was probed by stepwise dilution of a solution of [**5**][$B(C_6F_5)_4$] in C_6D_5Br. The chemical shift difference between the *m*-F and *p*-F resonances ($\Delta(\delta_{m,p\text{-F}})$, 4.2 ppm in the free anion) changes from 0.5 ppm (37 mM) to 2.4 ppm (3.7 mM) and 3.7 ppm (0.37 mM), respectively, upon dilution. This behavior suggests that contact ion pair [**5**][$B(C_6F_5)_4$] is in fast equilibrium with a solvent-separated ion pair [**5**·C_6D_5Br]-[$B(C_6F_5)_4$].

Conclusions

The introduction of an *N*,*N*-dimethylaminoethyl substituent on one of the nitrogen atoms of amidinate ligands reduced the tendency of (amidinate)Fe(II) chloro complexes to decompose through ligand redistribution. At the same time, the decreased steric demand of the substituent has restored the tendency of the amidinate to bridge two metal centers. Nevertheless, this did allow the synthesis of the diiron dibenzyl complex [(μ-^{Si}L)$FeCH_2Ph]_2$ (**4**), with 14 VE per Fe center.

Abstraction of one of the benzyl groups in **4** by Lewis or Brønsted acids gives rise to the paramagnetic diiron monocation [(μ-^{Si}L)$_2Fe_2CH_2Ph]^+$ ($\mathbf{5}^+$) partnered with weakly coordinating (fluoroaryl)borate anions. Weak cation−anion interactions in these ion pairs in C_6D_5Br solution were readily detected by ^{19}F NMR spectroscopy, due to the paramagnetic nature of the cation, although it is difficult to establish the precise nature of the contact interaction between cation and anion.

Experimental Section

Instrumentation. NMR spectra were recorded on Varian Inova 500, VXR 300, and Varian Gemini 200 instruments. ^1H chemical shifts are referenced to residual protons in deuterated solvents and are reported relative to tetramethylsilane. IR spectra were recorded on a Mattson 4020 Galaxy FT-IR spectrometer. GC-MS analyses were conducted using a HP 5973 mass-selective detector attached to a HP 6890 GC instrument. Elemental analyses were performed by the Microanalytical Department at the University of Groningen or by Mikroanalytisches Laboratorium H. Kolbe, Mülheim an der Ruhr, Germany. Reported values are the averages of two independent determinations. ES-MS spectra were obtained using a Nermag R3010 triple quadrupole MS system with a custom-built IonSpray (pneumatically assisted electrospray) source.[24] A JEOL JMS600 spectrometer was used for exact mass determinations. Magnetic susceptibility measurements were performed on microcrystalline samples (ca. 25 mg) using a Quantum Design MPMS-7 SQuID

(22) Addition of excess $PhNMe_2$ to a C_6D_5Br solution of [**5b**][$B(C_6F_5)_4$], generated from **4b** and $[Ph_3C][B(C_6F_5)_4]$, does not result in a significant increase in $\Delta\delta_{(m,p\text{-F})}$ or in smaller linewidths in the ^{19}F NMR spectrum.

(23) Zuccaccia, C.; Stahl, N. G.; Macchioni, A.; Chen, M.-C.; Roberts, J. A.; Marks, T. J. *J. Am. Chem. Soc.* **2004**, *126*, 1448.

(24) Bruins, A. P.; Covey, T. R.; Henion, J. D. *Anal. Chem.* **1987**, *59*, 2642.

magnetometer. Samples were contained in sealed NMR tubes, which were inserted in a plastic straw. The data were corrected for diamagnetism using tabulated Pascal's constants.[25]

General Considerations. All experiments were carried out under a dry dinitrogen atmosphere using Schlenk and drybox techniques. Toluene, pentane, diethyl ether, and THF were distilled from Na or Na/K alloy before use or purified by percolation under nitrogen atmosphere over columns of alumina, molecular sieves, and supported copper oxygen scavenger (BASF R3-11). Benzene-d_6 and THF-d_8 were dried over Na/K alloy and vacuum transferred before use. Bromobenzene-d_5 was degassed and dried over CaH_2.

Starting Materials. Anhydrous $FeCl_2$,[26] $B(C_6F_5)_3$,[27] and KCH_2-Ph[28] (from *n*BuLi, KO*t*Bu, and toluene) were prepared following literature procedures. $[Ph_3C][B(C_6F_5)_4]$ (Strem) and $[PhNHMe_2]$-$[B(C_6F_5)_4]$ (Asahi Glass Co.) were commercial products and were used without further purification. The amidine ^{Ar}LH was deprotonated *in situ* (*n*BuLi/THF) to give the lithium amidinate Li[^{Ar}L]. Lithium amidinate Li[^{Si}L] was prepared according to a literature procedure.[7]

***N*-(2,6-Diisopropylphenyl)-*N*′-(2-dimethylaminoethyl)benzamidine (^{Ar}LH).** *N*-(2,6-Diisopropylphenyl)benzimidoyl chloride[29] (30 g, 0.10 mol) was added to a solution of *N*,*N*-dimethylethylenediamine (22.0 mL, 0.20 mol) in toluene (150 mL). After refluxing for 1 h the mixture was cooled and 2 N KOH (330 mL) was added. The organic phase was washed with water, dried with Na_2SO_4, and concentrated. The concentrate was distilled using a Kugelrohr apparatus (200 °C, 0.02 mmHg) to give 28.1 g (0.080 mol, 80.0%) of ^{Ar}LH (mixture of isomers) as a pale yellow, slowly solidifying oil. ^{1}H NMR (200 MHz, $CDCl_3$, 25 °C): δ 6.7−7.9 (m, 8H, ArH), 4.8−5.2 (s, 1H, NH), 3.4−3.6 (s, 2H, CH_2), 2.9−3.1 (s, 2H, *i*Pr-CH), 2.4−2.6 (s, 2H, CH_2), 1.9−2.3 (s, 6H, CH_3, NCH_3), 0.8−1.3 (m, 6H, *i*Pr-CH_3), 0.6−1.4 (m, 6H, *i*Pr-CH_3) ppm. ^{1}H NMR (500 MHz, PhMe-d_8, 120 °C): δ 7.51 (s, 2H, ArH), 7.02−7.15 (m, 6H, ArH), 4.98 (s, 1H, NH), 3.40 (s, 2H, CH_2), 3.34 (septet, J = 6.7 Hz, 2H, *i*Pr-CH), 2.35 (s, 2H, CH_2), 2.12 (s, 6H, NCH_3), 1.36 (s, 6H, *i*Pr-CH_3), 1.22 (s, 6H, *i*Pr-CH_3) ppm. ^{13}C{^{1}H} NMR (125 MHz, $CDCl_3$, RT): δ 156.3 (Ar−C_{ipso}), 153.9 (Ar−C_{ipso}), 145.3 (Ar−C_{ipso}), 143.8 (Ar-C_{ipso}), 139.0 (Ar−C_{ipso}), 138.1 (Ar−C_{ipso}), 136.2 (Ar−C_{ipso}), 134.9 (Ar-C_{ipso}), 129.0 (Ar-CH), 128.1 (Ar-CH), 127.7 (Ar-CH), 126.7 (Ar-CH), 122.9 (Ar-CH), 122.4 (Ar-CH), 122.0 (Ar-CH), 59.0 (CH_2), 58.1 (CH_2), 46.0, 45.1 (*i*Pr-CH), 41.6 (CH_2), 40.7 (CH_2), 39.2 (CH_2), 28.8 (*i*Pr-CH_3), 28.4 (*i*Pr-CH_3), 27.6 (*i*Pr-CH_3), 27.5 (*i*Pr-CH_3), 23.6 (*i*Pr-CH_3), 22.4 (*i*Pr-CH_3). All signals broadened. IR (KBr): $\tilde{\nu}$ 2959 (s), 2866, 2820, 2772 (w), 1630 (s), 1603, 1588, 1578(w), 1499, 1479, 1462, 1445 (m), 1381, 1360, 1300, 1256, 1057, 1042 (w), 774, 762, 700 (m) cm^{-1}. HRMS (EI): calcd for $C_{23}H_{33}N_3$ 351.2674; found 351.2671.

[(μ-^{Ar}L)FeCl]$_2$ (1a). Li[^{Ar}L] (1.0 g, 2.8 mmol) and $FeCl_2$ (0.37 g, 2.9 mmol) were stirred in THF (30 mL) for 20 min. The solvent was removed *in vacuo*. Any residual THF was removed by stirring the reaction mixture in pentane (20 mL) and subsequently pumping off the volatiles (2×). The resulting green-gray powder was washed with pentane until the pentane was nearly colorless. The residue was extracted with toluene until the toluene was colorless. The combined toluene extracts were concentrated to ca. 50%. Warming to 80 °C and subsequent cooling to room temperature afforded dark yellow crystals. Yield: 0.51 g (0.58 mmol, 40%). ^{1}H NMR (500 MHz, C_6D_6, RT): δ ($\Delta\nu_{1/2}$) 106.8 (4500 Hz, 6H), 22.7 (66 Hz, 2H), 19.7 (540 Hz, 2H), 5.7 (29 Hz, 1H), 4.4 (58 Hz, 2H), −3.5 (84 Hz, 6H), −20.9 (870 Hz, 6H), −26.3 (54 Hz, 1H), −32.6 (1100 Hz, 2H) ppm. IR (Nujol mull, KBr): $\tilde{\nu}$ 1504 (m), 1484, 1461, 1388, 1379 (s), 1349 (m), 1312, 1276, 1262, 1257, 1057, 927 (w), 785 (m), 768 (w), 703 (m), 431 (w) cm^{-1}. Anal. Calcd for $C_{46}H_{64}N_6Cl_2Fe_2$ (883.65): C 62.53, H 7.30, N 9.51, Cl 8.02, Fe 12.64. Found: C 62.55, H 7.61, N 9.40, Cl 7.50, Fe 12.46.

[(μ-^{Si}L)FeCl]$_2$ (1b). A solution of Li[^{Si}L] (8.92 g, 33.1 mmol) in THF (30 mL) was added dropwise to a stirred suspension of $FeCl_2$ (4.20 g, 33.1 mmol) in THF (20 mL) at −40 °C. The reaction mixture was stirred for an additional 30 min at room temperature. THF was removed under reduced pressure, and residual THF was removed by stirring the pale yellow solid in pentane (50 mL) and pumping off all volatiles under vacuum. Continuous extraction with CH_2Cl_2 (100 mL) yields a dark yellow solution. The extract was evaporated to dryness, and the residue was washed with THF (50 mL, 3×), yielding a pale yellow solid. Yield: 7.51 g (10.6 mmol, 64%). ^{1}H NMR (500 MHz, CD_2Cl_2, RT δ ($\Delta\nu_{1/2}$, integral)): 327.0 (2130 Hz, 2H, CH_2), 175.1 (1820 Hz, 2H, CH_2), 115.3 (670 Hz, 6H, NMe_2), 110.5 (990 Hz, 2H, CH_2), 68.5 (640 Hz, 6H, NMe_2), 42.4 (790 Hz, 2H, CH_2), 35.1 (490 Hz, 2H, *m*-H_{Ph}), 18.1 (490 Hz, 2H, *m*-H_{Ph}), 5.1 (270 Hz, 18H, $SiMe_3$), 2.2 (47 Hz, 2H, *p*-H_{Ph}) ppm. IR (Nujol mull, KBr): $\tilde{\nu}$ 3054 (m), 2797, 1579 (w), 1501, 1484, 1393, 1333 (s), 1281 (w), 1246 (s), 1174 (m), 1155, 1100 (w), 1076 (m), 1056 (w), 1036, 1022, 952, 939 (m), 862, 845 (s), 796, 779, 768, 737, 724, 704 (m), 653, 635, 589, 580, 530, 461, 452, 437, 427, 415 (w) cm^{-1}. Anal. Calcd for $C_{28}H_{48}N_6Si_2Cl_2Fe_2$ (707.50): C 47.53, H 6.84, N 11.88, Cl 10.02, Fe 15.79. Found: C 47.49, H 6.70, N 11.97, Cl 10.06, Fe 15.67.

(^{Ar}L)$_2$Fe (2). A mixture of $FeCl_2$ (0.39 g, 3.03 mmol) and Li[^{Ar}L] (2.17 g, 6.06 mmol) was dissolved in THF (25 mL). The reaction mixture was stirred for 2 h at room temperature, and the solvent was removed *in vacuo.* The residue was extracted with diethyl ether, and the solvent was subsequently removed *in vacuo.* After addition of pentane (15 mL) to the product a white solid precipitated. The pentane was decanted. The product was obtained as dark yellow crystals after recrystallization from hot toluene. Yield: 1.1 g (1.5 mmol, 50%). ^{1}H NMR (300 MHz, C_6D_6, 25 °C): δ ($\Delta\nu_{1/2}$) 133 (67 Hz),118 (762 Hz), 98 (706 Hz), 83 (850 Hz), 70, 16.6, 15.7 (54 Hz), 9.4 (37 Hz), 8.8 (64 Hz), 6.9, 5.8, 5.6, 5.0, 4.1, 3.6, 2.5, 2.2, 1.2, 1.1, 0.9, −1.1 (74 Hz), −4.0 (39 Hz), −5.3 (331 Hz), −7.0 (78 Hz), −7.7 (78 Hz), −8.6 (70 Hz), −13.2 (85 Hz), −18.8 (218 Hz) ppm. IR (Nujol mull, KBr): $\tilde{\nu}$ 1590 (w), 1578 (m), 1550 (s), 1488 (w), 1464 (m), 1318 (m), 1218 (w), 1252 (w), 1137 (w), 1073 (m), 1057 (w), 953 (w), 907 (w), 780 (m), 764 (w), 752 (w), 701 (m) cm^{-1}. Anal. Calcd for $C_{46}H_{64}N_6Fe$ (756.90): C 73.00, H 8.52, N 11.10. Found: C 72.88, H 8.49, N 10.87.

[$Me_2NCH_2CH_2NC(Ph)N(2,6$-*i*$Pr_2C_6H_3)C(O)$]FeCl(CO)$_2$ (3). A solution of **1a** (0.50 g, 0.57 mmol) in toluene (15 mL) was degassed by three freeze−pump−thaw cycles. Excess CO (1 atm) was admitted, and the reaction mixture was stirred at room temperature for 2 days. Toluene was removed *in vacuo*, and the residue was extracted with pentane until the pentane was colorless. Concentration of the extract and cooling to −80 °C afforded yellow needles. Yield: 0.48 g (0.46 mmol, 81%). ^{1}H NMR (300 MHz, C_6D_6, 25 °C): δ 7.10−6.79 (m, 8H, ArH), 4.07 (septet, $^3J_{HH}$ = 6.6 Hz, 1H, CH), 3.07 (m, 4H, CH_2 + CH), 2.36 (s, 3H, NCH_3), 2.06 (s, 3H, NCH_3), 1.52 (d, $^3J_{HH}$ = 6.3 Hz, 3H, CH_3), 1.35 (d, $^3J_{HH}$ = 6.6 Hz, 3H, CH_3), 1.22 (m, $^3J_{HH}$ = 6.9 Hz, 4H, CH_3 and CH_2), 1.07 (d, Hz $^3J_{HH}$ = 6.9 Hz, 3H, CH_3) ppm. ^{13}C{^{1}H} NMR (50 MHz, C_6D_6, 25 °C): δ 208.1, 207.9 and 207.5 (CO), 164.1 (NCN), 147.6 (C_{ipso}Ar), 144.6 (C_{ipso}Ph), 132.2 (C_{Ar}*i*Pr), 128.6, 127.8, 126.1, 125.6, 122.5 and 121.2 (C_{Ar}H), 60.0 (CH_2), 51.2 and 49.3 (NCH_3), 48.0 (CH_2), 27.8 and 26.7 (CH), 24.6, 24.1, 21.3, and 20.8 (CH_3) ppm. IR (Nujol mull, KBr): $\tilde{\nu}$ 2073 (s, C≡O), 1949 (s, C≡O), 1669 (s, C═O), 1639 (m), 1463 (s), 1327 (m), 1268, 1022 (w), 990 (mw), 946 (w), 805 (mw), 786 (w), 769, 713 (mw), 674, 489, 467, 430 (w) cm^{-1}.

(25) Kahn, O. *Molecular Magnetism;* Wiley-VCH: New York, 1993; p 3.
(26) Kovacic, P.; Brace, N. O. *Inorg. Synth.* **1960**, *6*, 172.
(27) Pohlmann, J. L. W.; Brinckmann, F. E. *Z. Naturforsch.* **1965**, *20b*, 5.
(28) Lochmann, L.; Trekoval, J. *J. Organomet. Chem.* **1987**, *326*, 1.
(29) Nijhuis, C. A.; Jellema, E.; Sciarone, T. J. J.; Meetsma, A.; Budzelaar, P. H. M.; Hessen, B. *Eur. J. Inorg. Chem.* **2005**, 2089.

Anal. Calcd for $C_{26}H_{32}N_3O_3ClFe$ (525.86): C 59.39, H 6.13, N 7.99, Cl 6.74, Fe 10.62. Found: C 59.28, H 6.20, N 8.09, Cl 6.74, Fe 10.83.

[(μ-^{Si}L)FeCH$_2$Ph]$_2$ (4). A suspension of [(μ-^{Si}L)FeCl]$_2$ (**1b**) (3.34 g, 4.72 mmol) and KCH$_2$Ph (1.23 g, 9.44 mmol) in THF (30 mL) was allowed to warm from −40 °C to room temperature while stirring. The resulting yellow solution was stirred for an additional hour at room temperature. THF was evaporated under vacuum. Residual THF was removed by stirring the solid residue in pentane (50 mL) and pumping off all volatiles. The residue was extracted (6×) with diethyl ether (150 mL), and the extract was evaporated to dryness, yielding a yellow powder. Recrystallization from hot (80−100 °C) toluene (20 mL) afforded red crystals. Yield: 1.68 g (2.1 mmol, 43%). ^{1}H NMR (500 MHz, C_6D_6, RT): δ 189.7 (681, 2H, CH_2), 123.4 (878, 4H, CH_2), 92.8 (939, 2H, CH_2), 77.3 (1269, 6H, NMe), 30.4 (388, 4H, *m*-H_{Bz}), 22.1 (501, 4H), 17.1 (707, 2H), 14.4 (612, 4H), 6.7 (586, 18H, $SiMe_3$), −41.2 (601, *o*-H_{Ph}), −60.0 (391, 2H, *p*-H_{Bz}) ppm. IR (KBr, nujol): $\tilde{\nu}$ 3066, 3049, 3013, 1590 (m), 1497, 1480 (s), 1390, 1370 (m), 1335 (s), 1299 (w), 1257, 1244, 1214, 1170, 1075 (m), 1039 (w), 1019 (m), 951, 859, 836 (s), 794, 779, 759, 744, 722, 697 (m), 637, 625, 579, 544 (w), 520 (m), 405 (w) cm^{-1}. Anal. Calcd for $C_{42}Fe_2H_{62}N_6Si_2$ (818.86): C 61.61, H 7.63, N 10.26, Fe 13.64. Found: C 61.04, H 7.62, N 10.26, Fe 13.51.

Generation of [5][PhCH$_2$B(C$_6$F$_5$)$_3$] and Reaction with Pyridine-*d*$_5$. B(C_6F_5)$_3$ (12.5 mg, 24.4 μmol) was added to a solution of **4** (20 mg, 24.4 μmol) in C_6D_5Br (0.5 mL). A dark red solution was obtained. ^{19}F NMR (188 MHz, C_6D_5Br, RT): δ −126.4 ($\Delta\nu_{1/2}$ 111.4 Hz, 6F, *o*-F), −159.7 ($\Delta\nu_{1/2}$ = 138.9 Hz, 6F, *m*-F), −161.0 ($\Delta\nu_{1/2}$ = 85.5 Hz, 3F, *p*-F) ppm. Addition of 3 drops of pyridine-d_5 to the NMR tube resulted in a yellow solution. ^{19}F NMR (188 MHz, C_6D_5Br, RT): δ −129.7 (d, 20 Hz, 6F, *o*-F), −163.3 (t, 19 Hz, 3F, *p*-F), −165.6 (m, 6F, *m*-F) ppm. ES-MS (70 eV, THF): neg-ion mode, *m*/*z* 167 [C_6F_5]$^-$ (35%), 435 [$PhCH_2BH(C_6F_5)_2$]$^-$ (30%), 512 [$B(C_6F_5)_3$]$^-$ (15%), 603 [$PhCH_2B(C_6F_5)_3$]$^-$ (100%).

Generation of [5][B(C$_6$F$_5$)$_4$] from 4 and [Ph$_3$C][B(C$_6$F$_5$)$_4$] and Reaction with Pyridine-*d*$_5$. An orange solution of [Ph_3C][$B(C_6F_5)_4$] (28.2 mg, 30.5 μmol) in C_6D_5Br (0.5 mL) was added to **4** (25.0 mg, 30.5 μmol). A dark red solution was obtained. ^{19}F NMR (188 MHz, C_6D_5Br, RT): δ −129.2 ($\Delta\nu_{1/2}$ = 71.8 Hz, 4F, *o*-F), −159.2 ($\Delta\nu_{1/2}$ = 78.4 Hz, 4F, *p*-F), −159.9 ($\Delta\nu_{1/2}$ = 81.5 Hz, 8F, *m*-F) ppm. Addition of 3 drops of pyridine-d_5 to the NMR tube resulted in a yellow solution. ^{19}F NMR (188 MHz, C_6D_5Br, RT): δ −131.1 ($\Delta\nu_{1/2}$ = 42.4 Hz, 8F, *o*-F), −161.4 ($\Delta\nu_{1/2}$ = 47.3 Hz, 4F, *p*-F), −164.6 ($\Delta\nu_{1/2}$ = 51.4 Hz, 8F, *m*-F) ppm.

Generation of [5][B(C$_6$F$_5$)$_4$] from 4 and [PhNHMe$_2$][B(C$_6$F$_5$)$_4$] and Reaction with Pyridine-*d*$_5$. Benzyl complex **4** (25.0 mg, 30.5 μmol) was dissolved C_6D_5Br (0.5 mL). [$PhNHMe_2$][$B(C_6F_5)_4$] (24.5 mg, 30.5 μmol) was added to this solution. ^{19}F NMR (188 MHz, C_6D_5Br, RT): δ −129.7 ($\Delta\nu_{1/2}$ = 61.1 Hz, 8F, *o*-F), −160.2 ($\Delta\nu_{1/2}$ = 62.1 Hz, 4F, *p*-F), −161.1 ($\Delta\nu_{1/2}$ = 77.0 Hz, 8F, *m*-F) ppm. Three drops of pyridine-d_5 were added to the NMR tube. ^{19}F NMR (188 MHz, C_6D_5Br, RT): δ −131.1 ($\Delta\nu_{1/2}$ = 40.7 Hz, 8F, *o*-F), −161.7 ($\Delta\nu_{1/2}$ = 45.2 Hz, 4F, *p*-F), −165.0 ($\Delta\nu_{1/2}$ = 49.0 Hz, 8F, *m*-F) ppm.

Dilution Experiment with [5][B(C$_6$F$_5$)$_4$]. [Ph_3C][$B(C_6F_5)_4$] (16.9 mg, 18.3 μmol) was added to a solution of **4** (15 mg, 18.3 μmol) in C_6D_5Br (0.5 mL). A dark red solution was obtained. ^{19}F NMR (188 MHz, C_6D_5Br, 37 mM, RT): δ −129.4 ($\Delta\nu_{1/2}$ = 55.2 Hz, 8F, *o*-F), −160.0 ($\Delta\nu_{1/2}$ = 55.7 Hz, 4F, *p*-F), −160.5($\Delta\nu_{1/2}$ = 69.7 Hz, 8F, *m*-F) ppm. From this solution was taken 50 μL, which was diluted with C_6D_5Br (450 μL). ^{19}F NMR (188 MHz, C_6D_5Br, 3.7 mM, RT): δ −129.8 ($\Delta\nu_{1/2}$ = 43.9 Hz, 8F, *o*-F), −161.2 ($\Delta\nu_{1/2}$ = 47.8 Hz, 4F, *p*-F), −163.6 ($\Delta\nu_{1/2}$ = 52.7 Hz, 8F, *m*-F) ppm. From this solution was taken 50 μL, which was diluted with C_6D_5Br (450 μL). ^{19}F NMR (188 MHz, C_6D_5Br, 0.37 mM, RT): δ −132.0 ($\Delta\nu_{1/2}$ = 66.0 Hz, 8F, *o*-F), −161.8 ($\Delta\nu_{1/2}$ = 80.2 Hz, 4F, *p*-F), −165.5 ($\Delta\nu_{1/2}$ = 114.5 Hz, 8F, *m*-F) ppm.

X-ray Structure Deteminations. Crystal, collection, and refinement data for complexes **1a**, **1b**, **2**, **3**, and **4** are listed in Tables S1 and S2 (Supporting Information). Illustrations were prepared with the program PLATON.[30]

1a: Crystals were obtained by slow cooling of a hot (80 °C) toluene solution.

1b: Crystals were obtained by recrystallization from dichloromethane. Refinement was complicated by rotational disorder in the trimethylsilyl fragment (C12−C14) and conformational disorder in the C1, C2, and C3 positions of the chelate ring. A disorder model with site occupancy factor refinement was applied. The C1−C3 fragment was refined to two conformations with sof's of 0.57 and 0.43. The $SiMe_3$ methyls were refined to two positions with sof's of 0.52 and 0.48. In the subsequent refinement bond restraints for the Si−C distances were applied. A difference Fourier synthesis resulted in the location of the hydrogen atoms of the phenyl group. The remaining hydrogen atoms were included in the final refinement riding on their carrier atoms.

2: Crystals were obtained by recrystallization from pentane.

3: Crystals of composition **3**·2THF were obtained by recrystallization from THF. Refinement was complicated by disorder/partial occupancy of both the THF solvent molecules, which did not refine satisfactorily. The BYPASS[31] procedure was used to take into account the electron density in the potential solvent area, which resulted in an electron count of 175 in a volume of 1072.4 Å^3 in the unit cell. (Meaning the site occupation factor for the enclosed THF molecules is 0.55.)

4: Crystals were obtained by slow cooling of a hot (80 °C) toluene solution to room temperature. Refinement was complicated by conformational disorder in the benzyl fragments (C152−C212). A disorder model with two conformations of the benzyl ligand (refined to sof's of 0.44 and 0.56, respectively) was introduced with "variable metric" rigid group restraints in the refinement. A difference Fourier synthesis resulted in the location of all the hydrogen atoms, of which the coordinates and isotropic displacement parameters were refined, except those belonging to disordered C atoms of the benzyl ligand. The remaining hydrogen atoms were generated by geometrical considerations and refined in the riding mode. The adp of C152 converged to nonpositive definite displacement parameters when allowed to vary anisotropically, so ultimately this was reset to an isotropic displacement factor.

Acknowledgment. This work is part of the Research Programme of the Dutch Polymer Institute (DPI), project no. #110.

Supporting Information Available: ^{1}H NMR spectrum of **4**. Magnetic susceptibility data for complexes **1** and **4**. Crystallographic data for compounds **1a**, **1b**, **2**, **3**, and **4** (CIF). This material is available free of charge via the Internet at http://pubs.acs.org.

OM701155B

(30) (a) Spek, A. L. PLATON, Program for the automated analysis of molecular geometry (A multipurpose crystallographic tool); University of Utrecht: The Netherlands, 2002. (b) Spek, A. L. *Acta Crystallogr. A* **1990**, *46*, C34.

(31) Sluis, P.; Van der; Spek, A. L. *Acta Crystallogr. A* **2005**, *46*, 194.